

# Generation of Nitrogen Emission Line at 337 nm in the Laboratory and at High Altitudes

Mladen M. Kekez 

**Abstract**—This paper consists of two parts. In the first part, the emission was generated in air, and the waveform recording the spectral line at 337 nm (= prominent N<sub>2</sub> laser line) was noted. The pulse forming network (PFN) Marx generator having a large (50 Ω) internal impedance was used. The pulses of the nitrogen emission at 337.1 nm of long (<3 μs) duration and of short (≈10 ns) duration were obtained. The photodiode registered both the spontaneous emission and the stimulated (laser) emission in the 337 ± 5 nm spectral range. The data show that the laser emission predominates in the pulses of long duration. In the second part of this paper, it is suggested that the ultraviolet (UV) radiations emitted by the sun, together with the electric fields present at high altitudes, are capable of exciting the N<sub>2</sub> molecules to the upper excited C<sup>3</sup>Π<sub>u</sub> level to yield the laser emission of long duration. On the basis of the laser energy content dissipated into the plasma, the size of the transient luminous events (TLEs) known as the elves and the sprites was evaluated. The dynamics of initially small size, highly compressed, and very hot plasma formed inside the sprite was presented. It is proposed that the TLEs named “crepuscular twilight in the sky of New York” observed on December 28, 2018; “mysterious bright flash” occurred in Russia on January 9, 2018; and maybe the Tunguska event happened in Siberia on the morning of June 30, 1908 should be included in the list of the TLEs.

**Index Terms**—Coronas, elves and Tunguska event, nitrogen laser, plasma focus, spark channels, sprites, streamers.

## I. INTRODUCTION

CLASSICAL nitrogen laser is a gas laser which operates primarily in the ultraviolet (UV) range using molecular nitrogen. The highest output power is based on the transition of the second positive system of N<sub>2</sub>(C<sup>3</sup>Π<sub>u</sub>–B<sup>3</sup>Π<sub>g</sub>). The classical N<sub>2</sub> laser is pumped by an electrical discharge to create numerous filamentary streamer/corona channels in the glow-like discharge formed between the two parallel electrodes. The gas discharges formed in N<sub>2</sub> and/or air provides the N<sub>2</sub> laser gain medium. The preionization had to be applied to produce a semiuniform glow-like column [1]–[3]. The low (<1 Ω) impedance Blumlein transmission line driver was frequently used as the energy reservoir that has a short (<30 ns) transit time. The goal in designing the N<sub>2</sub> laser is to avoid the formation of the fully developed spark channels, which are mainly used in the operation of the rail gap switches for the

purpose of transferring the energy from a large condenser bank to the plasma load.

Using the Blumlein transmission line as the energy source, the classical N<sub>2</sub> laser operates with the voltages ranging from 8 to 14 kV and with the pressure between 70 and 250 torr of N<sub>2</sub>. The width of the laser pulses is <10 ns. The duration of the laser pulse as a function of pressure is proportional to the time interval of the voltage fall from the full value of the voltage supplied by the Blumlein driver to almost zero value. When such N<sub>2</sub> laser is made to operate at high (<760 torr) pressure, the excitation of the N<sub>2</sub> molecules and consequently the laser emission would yield only short duration pulses, from one nanosecond down to some tens of picoseconds.

From the research and development on the CO<sub>2</sub> lasers, it was learned that the transition from the glow-like discharge to the fully developed spark channel can be delayed if the internal impedance of the driver is of relatively large (>10 Ω) value. Note that the CO<sub>2</sub> laser given in [4] has evolved from the concept given in [5], and the uniform glow-like columns are the best laser gain medium for all the gas lasers.

The nine-stage Marx generator has 18-Ω internal impedance and it was used in [6]. The electromagnetic radiation pulses were observed both at the single microwave frequency close to 1 GHz and the pulses of long (<220 ns) duration at 337.1 nm (= prominent N<sub>2</sub> laser line) in the pressure range from 100 to 200 torr in nitrogen, and also in air, without the use of the laser resonator and the mirrors.

To further explore the importance of the impedance, eight-stage PFN Marx generator with 50-Ω internal impedance was employed in the current study. With this generator, it is expected that the new data on N<sub>2</sub> emission of long duration would be obtained, and this would facilitate the possibility of reaching some understanding of the N<sub>2</sub> lasing action at high altitudes.

At high altitudes, the transient luminous events (TLEs) take place. The TLEs include blue jets, elves, and sprites [7]. It is suggested herewith that the recent events named “crepuscular twilight in the sky of New York” recorded on December 28, 2018; “mysterious bright flash” occurred in Russia on January 9, 2018; and maybe the Tunguska event happened in Siberia on the morning of June 30, 1908 [8] should be included in the list of the TLEs.

The propagation mechanism for the constricted (filamentary) discharge is a matter of some physical interest. For example, Raizer *et al.* [9] and Inan [10] describe the onset criteria, the development of the streamer–leader channels at high altitudes, and their participation in the formation of

Manuscript received March 11, 2019; revised April 8, 2019; accepted April 29, 2019. Date of publication May 16, 2019; date of current version June 10, 2019. The review of this paper was arranged by Senior Editor F. Taccogna.

The author is with High-Energy Frequency Tesla Inc., Ottawa, ON K1H 7L8, Canada (e-mail: mkekez@magma.ca).

Color versions of one or more of the figures in this paper are available online at <http://ieeexplore.ieee.org>.

Digital Object Identifier 10.1109/TPS.2019.2914564

the TLEs. Raizer *et al.* [9] and Inan [10] contribute to our understanding regarding the electrical breakdown of gases, which was also described in detail in [11]. Furthermore, electron runaway plays a fundamental role in the electrical breakdown dynamics [12].

In [10], the mechanism of sprite formation was described as being caused by the release of intense electromagnetic pulses (EMPs) and because of the intense (quasi-static) electric fields present at high altitudes. They cause the heating of ambient electrons, ionization, and upward acceleration of relativistic runaway electrons leading to the formation of the sprites and elves.

In [13], the model is based on low-frequency RF breakdown of the upper atmosphere, ignited by the upward propagating electromagnetic pulses due to conventional low altitude lightning.

It is proposed here that the UV radiations emitted by the sun together with the electric field present in the mesosphere are capable of exciting the  $N_2$  molecules to the upper excited  $C^3\Pi_u$  level to yield the laser emission of long duration at high altitude.

The low altitude massive lightning (which are circa 0.5% compared to the total number of lightning strokes to the ground [13] and [14], and/or the manmade devices can provide the trigger pulse for the onset of the  $N_2$  laser action in the mesosphere.

The  $N_2$  laser pulse of a high-power value can be dissipated into the plasma via the detonation-like processes that have the full absorption of the laser beams with small absorption length. This process leads to the formation of the elves and the sprites. Following the detonation processes, the inward-going (embedded) shock is established due to the overextension of the hot gas because of the increase in the flow area. If the hydrogen would be present in the sprite, and if both the laser power and the electric field present at high altitudes are not of high values, it is expected that the thermonuclear reaction processes will not take place. However, there is only a small possibility of having the binary collisions between the two hydrogen molecules to produce the deuterium, neutrino, and the positron. When the laser pulse is of high power and at the same time the electrical fields are of high amplitude at high altitude, the thermonuclear processes could yield to the so-called Tunguska event.

In the first part of this paper, the generation of the  $N_2$  laser pulses of long duration was demonstrated in the laboratory. Because of this new information, the possibility of the generation of  $N_2$  laser emission of long duration could be considered to take place at high altitudes. The energy content of the laser beams dissipated into the plasma governs the size/dimensions of the elves and sprites. Later in time, the initially small size highly compressed and very hot plasma was formed inside the sprite. The dynamics of this small size plasma was presented in this paper.

## II. EXPERIMENTAL SETUP

In the experiments, the eight-stage pulse forming network (PFN) Marx generator (Fig. 1) produces the waveform shown

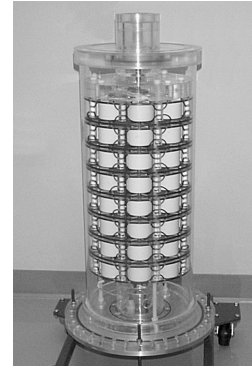


Fig. 1. Interior of eight-stage PFN Marx generator. The generator is placed in the aluminum tube of 12 inches diameter. The specifications of the generator are: ten capacitors per stage for a total of 80; capacitance per stage is 26 nF; charging voltage per stage varies from 12 to 28 kV; maximum stored energy in the system is 82 J; impedance of the load is 50  $\Omega$ ; coaxial structure was employed; and excellent reproducibility of the output pulse was achieved.

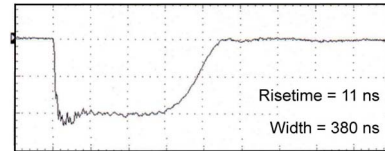


Fig. 2. Output: 50 kV/div.; 100 ns/div. generated by eight-stage PFN Marx generator. The waveform was measured with the aid of the voltage divider. The 18 in long, 50- $\Omega$  resistor was used as the load. When the capacitive probe was applied to measure the waveform of negative polarity, the rise time would fall to <4 ns.

in Fig. 2. The voltage impulse of negative polarity creates initially the filamentary corona/spark channel between the copper wire, which is attached to the central electrode 6 and the metallic electrode 5. The gap between the tip of the wire 6 and the metallic electrode 5 is circa 2 mm. The thimble 9 machined out of Plexiglas was placed over the polyethylene surface of RG 217/U coaxial cable. The height of the thimble above the upper edge of the conical structure 8 was 25 mm.

The diameter of the central electrode 7 in Fig. 3 was 15.9 mm with the height initially set to 55 mm and later to 80 mm. The metallic post was of 2.5 mm in diameter. The separation between the central electrode and the metallic post varied between 4 and 7 mm until the pulse of long duration was obtained. The precise alignment in the vertical direction was required so that the photodiode can view the glow-like discharges containing many filamentary channels that were formed between the central electrode 7 and the metallic post 5 or the nipple 4 when the metal post was removed

## III. DIAGNOSTICS

The diagnostic tools are Hamamatsu R 727 photodiode to record  $N_2$  emission at 337.1 nm Rogowski coil, and 3-GHz Tektronix oscilloscope: Model: TDS 694C to record the data.

Rogowski coil (= wideband current transformer), Model 110, is made by Pearson Electronics Inc., Palo Alto, USA, was inserted in the space between the points 10 and 11, indicated in Fig. 3.

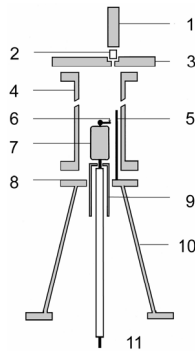


Fig. 3. Schematics of the experimental setup. 1—Hamamatsu R 727 photodiode. 2—337.1 nm bandpass filter of 11.8 mm diameter. 3—Plexiglas flange with the hole of 6.25 mm diameter and with the additional recess to accommodate the optical filter. 4— $2 \frac{3}{4}$ in (Varian) nipple. 5—Metallic post. 6—Copper wire attached to the central electrode. 7—Central electrode. 8—Upper edge of the conical structure. 9—Plexiglas thimble with the hole in the center machined to fit well the polyethylene insulation of the coaxial cable. 10—Conical structure connected to the ground of the Marx generator. 11—inner conductor of the coaxial cable with the connection to the generator.

Hamamatsu R 727 photodiode (of the rise time of  $<1$  ns), the 337.1-nm bandpass filter, was placed on top of the Plexiglas flange 3 shown in Fig. 3. The optical filter of 11.8 mm diameter was made by Edmund Optics, USA. The full width at half maximum (FWHM) of the filter is 10 nm. The hole of 6.25 mm was drilled in the Plexiglas cover 3, the “O” ring and 337-nm bandpass filter were placed on top of the hole. To avoid the interference problems as mentioned in [6], the laser signals recorded by the photodiode have been viewed with the aid of low (150 MHz)-pass filter.

#### IV. EXPERIMENTAL RESULTS

To obtain these results shown in Figs 4 and 5, many auxiliary studies have been done to understand why the Plexiglas thimble 9 had to be placed over the inner path of the polyethylene RG 217/U coaxial cable 11. Also, it was required to know why the impulse voltages from the eight-stage Marx generator had to have the first (voltage/current) pulse of negative polarity in the train of pulses produced.

Also, the relationship between the current and the emission at 337 nm had to be established. These auxiliary experiments will be given in a separate paper.

The result is shown in Fig. 4, and series #1 and #2, frame B, and the data shown in Fig. 5 were obtained with the following changes with respect to Fig. 3. The metallic post 5 was removed and the nipple 4 was moved toward the central electrode 7. Similarly, the nipple 4 was not any longer in a concentric position in regard to the central electrode 7. The separation between the central electrode 7 and the inner wall of the nipple 4 was varied until the relatively reproducible results of the high level of the emission were obtained.

The findings shown in Fig. 5 are in accord with the observation stated in [1], i.e., the details of the geometrical arrangement of the electrodes govern whether the stable emission will be occurring in their classical Blumlein  $N_2$  laser. In some of their arrangements, there was no emission, although the glow-like discharge was present between the electrodes.

In this paper, it was discovered that the initial filamentary channel between point 6 and the inner wall of the nipple 4 had to perform the following two functions: 1) to provide the preionization in the space between the central electrode 7 and the nipple 4 in order to have a glow-like column and 2) to provide incident signal of sufficient strength/number of photons needed for the onset of the stimulated (laser) emission. The discovery made regarding point #2 is more than one century old. Einstein [15] first broached the possibility of stimulated (laser) emission in 1917. He postulated that the photons prefer to travel together in the same state if one has a large collection of molecules containing a great deal of excess energy.

As mentioned in the caption of Fig. 4, frame C shows the waveform of the emission when the nipple 4 in Fig. 3 was replaced by 18.5-cm-long Plexiglas tube and the photodiode was placed on the tube or placed further away from the tube. With further work, it was learned how to enhance the emission and to get the reproducible data. These results are presented in Fig. 4, frame B series #2.

#### V. ADDITIONAL EXPERIMENTAL EVIDENCE

Before proceeding further, it may be advisable to consider the following discharges.

##### A. Lightning Discharges

The photograph of the lightning discharges originating below the cumulonimbus clouds to the ground is shown in Fig. 6, frame #1. The blue jet projecting above a thunderstorm to the lowest levels of the stratosphere, i.e., 40 to 50 km above the earth is also shown in Fig. 6, frame #1. The electrostatic energy stored in the cumulonimbus clouds supplies the energy required for the development of both the lightning and the blue jet. The main difference between these two phenomena is that they are developing under different conditions. It should be noted that the density of the air decreases exponentially upward from the surface of the earth with the scale of  $\sim 7$  km. For example, at ground level, the pressure is 760 torr and at 50 km the pressure falls to 0.16 torr. It could be suggested that the blue jet is just a self-arresting lightning discharge because the filamentary (spark) channel has difficulties to be established/maintained at low pressure and at a relatively modest value of the electrical fields.

Another point regarding the blue jet should be made. In the study of the microwave (maser) generation close to 1 GHz caused by the spark channel and corona discharges in air, the powerful hydrogen atom (maser) line at 1.420 GHz was recorded under the condition of high humidity present in the air [16]. This suggests that the driving frequency of high power at a frequency close to 1 GHz is capable of electrolysis of the water vapor present in the air, dissociation of the hydrogen molecule into atoms, excitation of atomic hydrogen, and consequent emission from the hydrogen atoms in the manner found in the hydrogen atomic clock.

As a consequence of the formation of the blue jets, the hydrogen atoms will be produced. Hydrogen being of a smaller mass in comparison to the other matters present in the

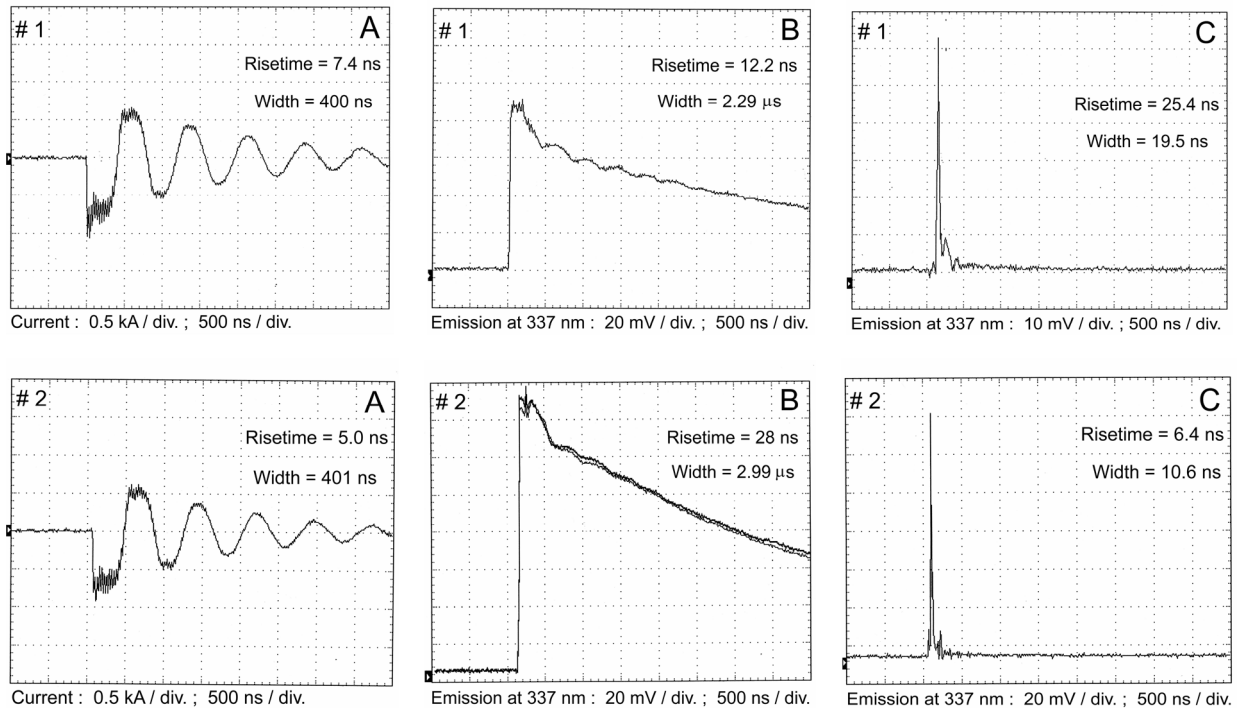


Fig. 4. Emission at 337.1 nm generated in air. Two series of data are presented. The experimental setup shown in Fig. 3 with some modifications presented in the text was used to get the series #1. With further work, it was learned how to enhance the emission and to get the reproducible data. These results are presented in series #2. Frame A shows the current waveform measured with the Rogowski coil. Frame B is the emission at 337 nm recorded with Hamamatsu R727 photodiode when the photodiode was placed close to the flange 3 in Fig. 3. Three consecutive waveforms of the emission are shown in frame B of series #2. Frame C gives the waveform of the emission when the nipple 4 in Fig. 3 was replaced by 18.5-cm-long Plexiglas tube, and the photodiode was placed on the Plexiglas tube or placed further away from the tube. To get short ( $\sim 10$  ns) duration pulses, the metallic post 5 was introduced back in the experimental setup. The generator was charged at 12.5 kV/stage. The word: “width” stated in frames A–C is for FWHM.

air will diffuse toward the mesosphere. Therefore, there are possibilities that ordinary hydrogen present in the mesosphere to be the raw material to yield the binary collisions between the two hydrogen molecules and to produce the deuterium, neutrino, and the positron in this low-yield thermonuclear fusion process. Deuterium, having the larger mass, will diffuse downward toward the clouds then rains down to the ocean. This may explain why deuterium has a natural abundance in the earth’s ocean and accounts for approximately 0.0156% (or, on a mass basis, 0.0312%) of all the naturally occurring hydrogen in the oceans.

### B. Sprite

The sprites (the acronym for stratospheric/mesospheric perturbations resulting from intense thunderstorm electrification) are apparently the most frequently observed of all the transient luminous events (TLEs) in the mesosphere.

The storms can produce 400–750 sprites within 4–5 h [7]. Two examples of sprites are shown in Fig. 6.

### C. Elve

The elves [the acronym for the emission of light for very low frequency (VLF)] perturbation from an electromagnetic pulse (EMP) source were recorded by the space shuttle low light camera. Red in color, an elve is a rapidly expanding disk triggered by the ground to cloud discharges. It occurs in the

range from 80 to 100 km. The diameter of the expanding disk can obtain a value of 400 km or even larger.

### D. Mysterious Flash Occurred in Russia

A mysterious bright flash shown in Fig. 8 produced the illumination over thousands of miles in Russia. It was stated that the explosion of light was accompanied by the “ground shaking.” The phenomenon was seen and felt over thousands of miles in Russia, but was especially evident in three regions: Bashkortostan, Udmurtia, and Tatarstan. Russian officials and scientists immediately denied that there had been a Russian missile test or any reported space rock crashing to Earth.

Such “bright event” was also recorded by Nikola Tesla in his study at Wardenclyffe Tower, Long Island, USA, during 1901–1906 [17]. A bright event to the naked eye at night took place over a large area near the coastline of Long Island and over the sea. It was thought that this bright event had been caused by the electrical discharges triggered by his generator located at Wardenclyffe Tower. The photograph shown in Figs. 7 and 8 could be considered to be similar to the event caused apparently by Nikola Tesla.

### E. Tunguska Event

The Tunguska event was a large explosion that occurred in Siberia on the morning of June 30, 1908 [8]. Over 80 million trees were demolished over a vast area greater than

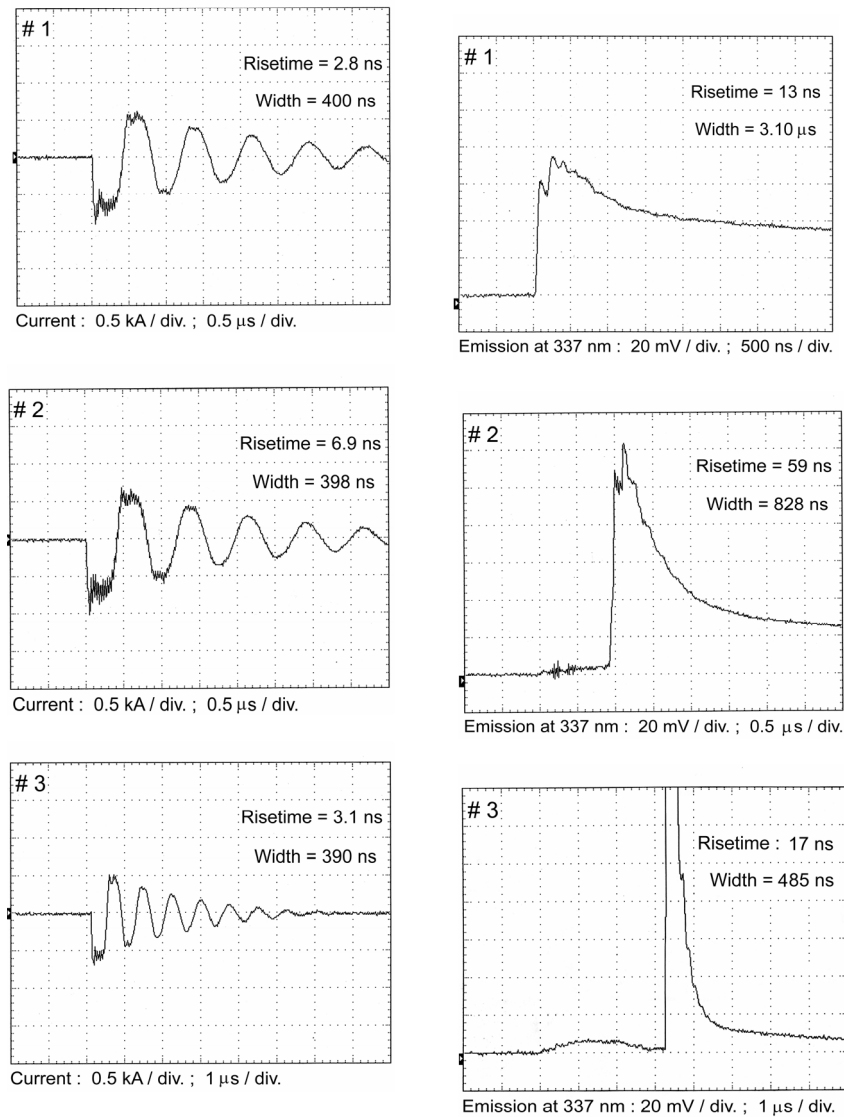


Fig. 5. Three shots of emission at 337.1 nm produced in air. The onset of the emission varies from shot to shot. In shot #1, the onset of the emission coincides with the onset of the current. There is a delay in the onset of the radiation in shots #2 and #3. It is suggested that in these two shots, the incident (triggering) signal was not of sufficient strength to facilitate the initiation of the emission as in shot #1. Some time is required for the incident signal to gain strength. Shots #2 and #3 have some feature of the Q-switched laser. The photodiode registered both the spontaneous emission and the stimulated (laser) emission in the  $337 \pm 5$  nm spectral range. This figure suggests that the laser emission predominates in the experimental setup used. The data shown in frames #2 and #3 were recorded from time to time. The data presented in this figure were recorded to get the series #1 of Fig. 4. The generator was charged at 12.5 kV/stage.

2000 square kilometers, yet caused no known human casualties. No crater was found nor anything that appeared to be the landing spot of whatever had caused the explosion. It is classified as the largest impact event on Earth in recorded history.

When the scaling laws from the effects of nuclear weapons evaluations were employed, the estimates of the energy of the airburst range from 3 to 5 megatons of TNT [= (12 to 20)  $10^{15}$ J]. The 15 megatons of TNT estimate represents the energy of about 1000 times greater than that of the atomic bomb dropped on Hiroshima, Japan.

## VI. THEORY

In the outer reaches of the earth environment, the solar electromagnetic radiation strikes the atmosphere with a power density of  $1370 \text{ W/m}^2$ , the value known as the “solar constant.”

For the whole earth (which has the diameter of 12715.43 km), the power received is  $1.740 \times 10^{17} \text{ W}$ .

The sun emits a significant amount of the UV radiation (about 10% of its total power) and the UV and shorter wavelengths are capable of dislodging an electron from a neutral gas molecule/atom during a collision via the process known as the photoionization. Also, the photoexcitation of a neutral molecule takes place. In addition to the UV radiation, the electrons, protons, and alpha particles blown toward the earth on the solar wind are dictating the earth environment. These radiations and the particles are absorbed mainly by nitrogen and they can pump the  $\text{N}_2$  molecules to the upper excited  $\text{C}^3\Pi_u$  level and at longer wavelengths, by simple diatomic oxygen. Most of the remaining UV in the midrange of energy is blocked by the ozone layer.

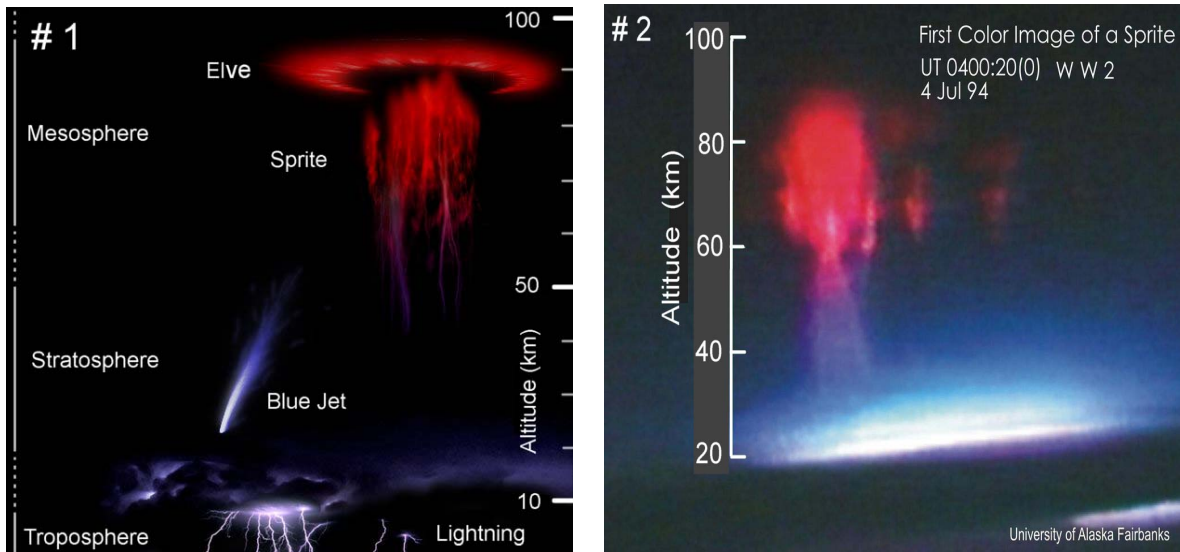


Fig. 6. Frame #1 is the representations of upper atmospheric lightning and electrical discharge phenomena. Frame #2 is sprite recorded by the University of Alaska Fairbanks, USA. (After <https://en.wikipedia.org>.)

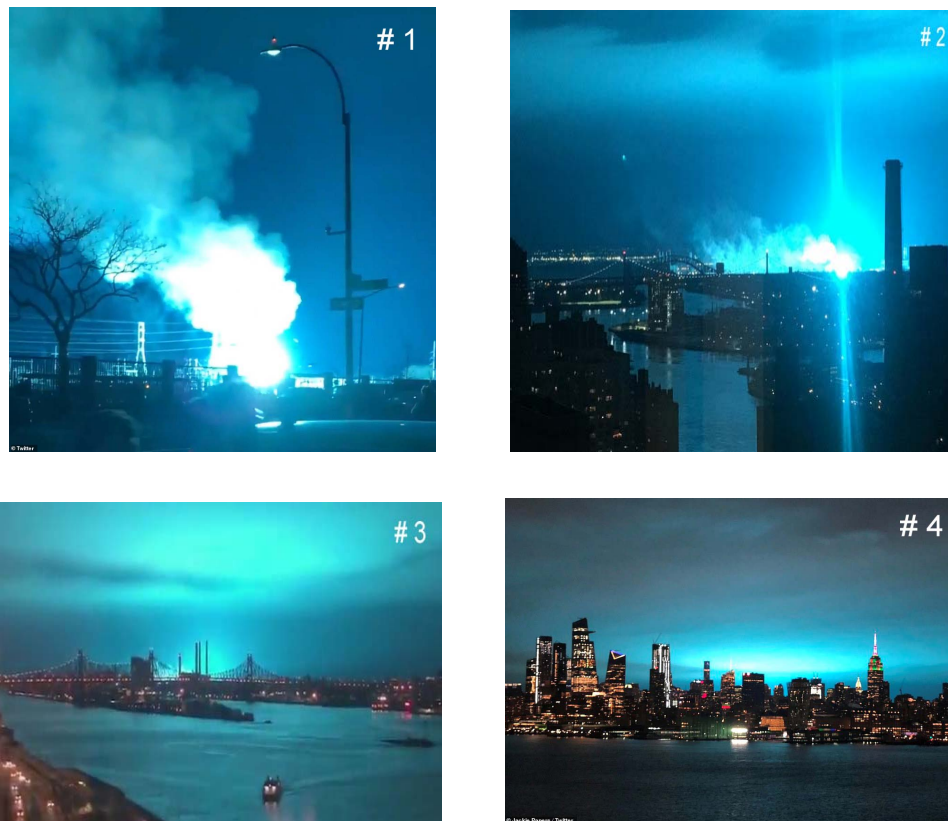


Fig. 7. Four still photographs of the “electrical arc flashes” that occurred over New York City on Friday, December 28, 2018. This event is named by the author “Crepuscular twilight in the sky of New York.” The initial “electrical arc flash” shown in frame #1 was caused by a Con. Ed. transformer explosion. Frame #2 indicates that the laser-like beams have emerged from the electric arc. It can be suggested that the beam propagating in the vertical direction has provided the incident (triggering) signal needed for the onset of the discharge processes occurring in the sky as shown in frames #3 and #4. The alternative explanation is that the incident (triggering) signal was provided by some lightning, and the laser-like beams shown in frame #2 were some stray light reflections hitting the camera.

The essential feature of the sprites and the elves, shown in Figs. 6–10, and perhaps the Tunguska event could be accounted for by considering the possibility of the laser action. An external electromagnetic pulse provides the triggering

signal (incident photons) required for the onset of the laser action. Without these external photons, the excited state of  $N_2$  molecules will decay via the spontaneous emission, hence creating the temperature profile across the mesosphere



Fig. 8. Snapshot of a mysterious bright flash turning night into day over a huge area in Russia. This snapshot was presented by the Russian TV channel #1 on January 9, 2018. This flash can be seen at: [https://www.youtube.com/watch?time\\_continue=10&v=81v-F59LYt0](https://www.youtube.com/watch?time_continue=10&v=81v-F59LYt0).

and giving the peak in temperature at 48 km above the earth.

For the onset of the laser radiation, the incident photons have to penetrate the ozone layer and reach the mesosphere that contains high-density numbers of the excited states of  $N_2$  molecules. After this initiation, the laser beams will be amplified as it propagates radially away from the ignition point. The amplification occurs because the UV radiation from the sun provides the excited states before the arrival of the upcoming laser beam, i.e., the sun performs the function of the xenon flash lamps that are used, for example, to pump the  $Nd^{3+}$ -doped phosphate glass laser in the system, like the one used in the U.S. National Ignition Facility (NIF). It should be noted that the NIF system delivers the UV laser pulse at 351 nm (= the third harmonic of 1053 nm) of the neodymium more than 1 ns.

To form the sprite, we could consider the case that the beams are converging back toward the ignition point. When the flux of the beams greatly exceeds the threshold value for the breakdown (measured in terms of the power per unit area), the gas is strongly ionized and the resultant plasma absorbs the laser beam as being heated furthermore to high temperatures.

Further evolution of the plasma could be accounted for from the gas-dynamics considerations. As suggested before, the plasma dynamics could be analogous to the propagation of a detonation wave in an explosive material [18], [19]. To proceed further, it is necessary to replace the reaction energy of the detonation with the laser energy of the incoming laser beams. For the detonation process of the spherical blast wave, the energy  $E$  is

$$E = [(R(t)^5 \rho_o)/t^2] * \text{constant}. \quad (1)$$

Expression (1) was derived by Taylor [18], [19] to account for the first explosion of an atomic bomb Trinity test in New Mexico, USA, in 1945. By using only photographs published in newspapers/magazines of the blast, G. I. Taylor had noted the value of the radius of the shock wave,  $R(t)$ , at particular time  $t$  and was able to estimate that the trinity explosion had released the energy of 25 kilotons of TNT. In the calculation, it was taken that the density for air at ground level,  $\rho_o$  is

$1.2 \text{ kg/m}^3$  and  $1 \text{ g of TNT} = 4 \text{ kJ}$ . He had also pointed out that the radiation losses escaping from the explosion were of the comparable value as the contribution to the energy addition due to the adiabatic index  $\gamma$ . He assumed the constant in (1) to be approximately 1.

Expression (1) is based on the Chapman–Jouguet condition for the detonations [20]

$$v^2 = [2(\gamma^2 - 1)]E_M \quad (2)$$

where  $v$  is the detonation velocity and  $E_M$  is the energy per unit of mass. For the cylindrical blast wave, the energy per unit length  $E_1$  of this blast wave is [21]

$$E_1 = [(R(t)^4 \rho_o)/[t^2(F(\gamma))^4] \approx [R(t)^4 \rho_o]/t^2 \quad (3)$$

where  $F(\gamma)$  is a slowly varying function of the adiabatic index  $\gamma$ , which can be taken as 1. When the unit length is considered to be equal to the radius  $R(t)$  in the definition of  $E_1$ , the expression (3) becomes identical to the expression (1).

Both the spherical blast wave and the cylindrical blast wave experience later the inward-going (embedded) shock due to the overextension of the hot gas by the increase in the flow area. For the cylindrical blast wave, the subsequent recompression takes place near the axis, generating a peak pressure at the axis that can be several times higher than the peak pressure of the original shock front [22]. For the spherical blast wave, the embedded shock wave moves toward the center of the sphere. During the recompression when the hydrogen is present, the thermonuclear reactions may take place in a rather small highly compressed volume of hydrogen. The lifetime of this high-temperature region is governed by the internal confinement plasma fusion conditions. Further processes that take place during the recompression will be stated later in this paper.

It could be suggested that the Tunguska detonation in Siberia was a successful laser-supported internal confinement fusion event. According to all the information available, the Tunguska detonation was not definitely due to the air burst of a meteoroid.

The overall dynamics of the plasma is complicated further by the presence of the Rayleigh–Taylor (R–T) instability. This instability occurs at the interface between two fluids of different densities, when the lighter fluid is pushing the heavier fluid, i.e., the expanding plasma is accelerated into the denser cold medium. In the vertical direction, we have a great change in the neutral gas density because the density of the air decreases exponentially upward from the surface of the earth with the scale of  $\sim 7 \text{ km}$ . Because of the R–T instability, the expansion of the hot gas downward will yield a filamentary structure of the sprite known as the tendrils, whereas the upward expansion will be defused as the neutral gas density is decreasing rapidly.

## VII. DISCUSSION

To some degree, the ideas presented above were examined already in the laboratory. When the powerful laser beam was brought to focus, the laser breakdown was generated and this was accompanied by a sharp explosive sound typical of



Fig. 9. Three photographs of sprite recorded above a storm on July 31, 2011, near Clovis, New Mexico, USA. (After: Chrissy Warrilow, weather.com.)

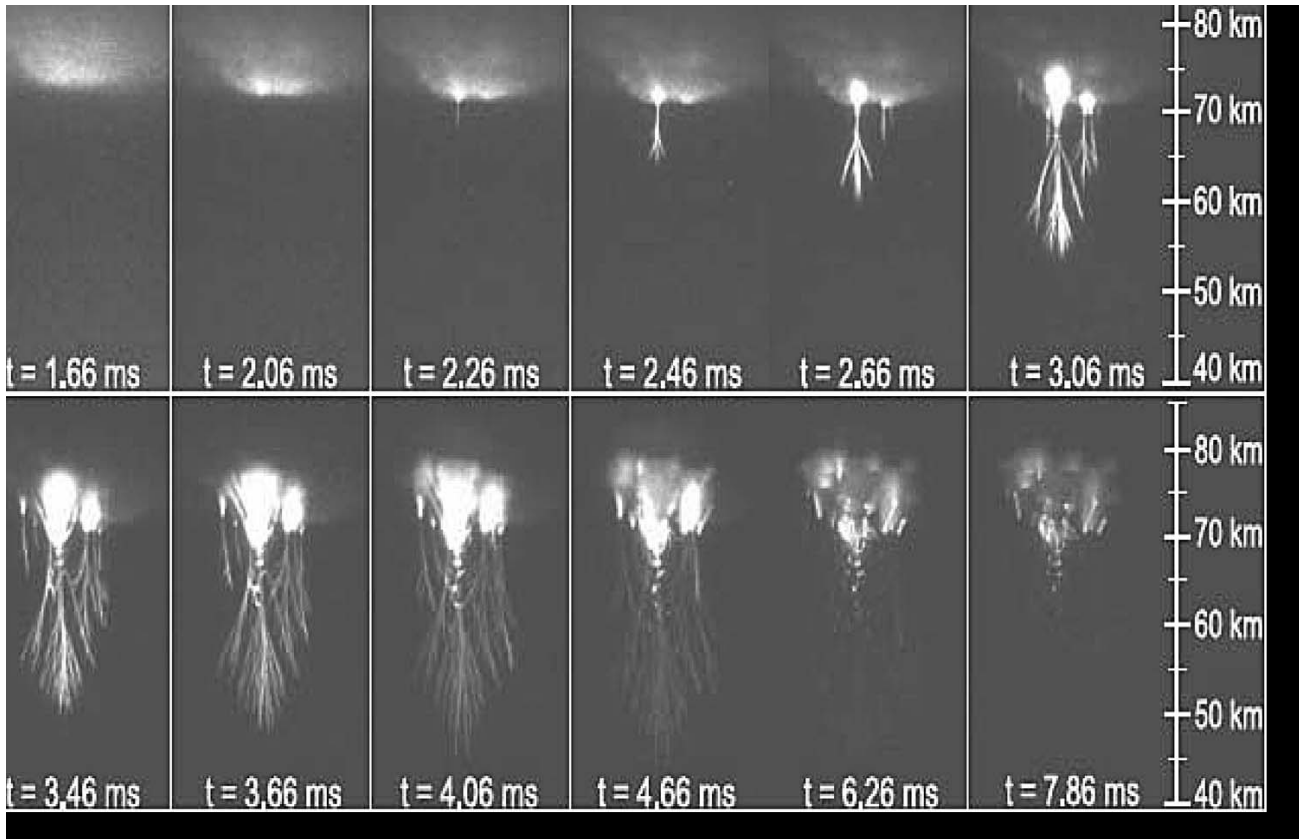


Fig. 10. High-speed images of red sprites (after Cummer *et al.* [27]). Reproduced by permission from The Geophysical Research Letters.

shock wave generation and the up-beam propagation of newly created plasma (named the laser spark) in the surrounding gas.

The experimental evidence related to the detonation velocity  $v$  can be obtained directly from (2).  $E_M$  is the energy per unit of mass and it is equal to  $E_M/(\rho_o \text{volume})$ . As the volume = (Area times  $(v \Delta t)$ ) =  $(\pi r_o^2(v \Delta t))$  and the laser energy  $E$  is the product of the power  $P$ , and the time interval  $\Delta t$ , we get

$$v = [2(\gamma^2 - 1) P / (\pi r_o^2 \rho_o)]^{1/3} \quad (4)$$

where  $\rho_o$  is the neutral gas density ahead and  $\gamma$  is the adiabatic index. A number of scientists have obtained that the velocity  $v$  increases as  $(P)^{1/3}$  and has made this mechanism most favored to date.

The 2-D records of the dynamics of the laser spark development were observed on the nanosecond time scale in [23]. The radial expansion of the laser spark was found to proceed with the velocity close to the sound velocity in the cold gas, and the laser (spark) channel expands approximately into a cone

of constant angle. There is also the evidence for a source of ionization traveling wave ahead of the plasma itself which is specified by a well-defined encircling shock wave front. These facts point out that the luminous picture of the laser plasma has the overall larger dimensions in comparison to what is expected from the detonation theory.

The laser spark structure produced in helium forms the plasma fireball, which was composed of a dense hot plasma core surrounded by a more tenuous halo. Later, the spherical shock velocity was measured to be fairly close to the velocity of sound in the cold background (helium) gas [24].

Using the two-wavelength interferometry, the 2-D profiles of the electron density were obtained throughout the evolution of the laser spark [25]. The development of the laser spark occurred as a result of a radiation-driven detonation wave of the type originally proposed in [26] and that the “two components” plasma structure (= the hot dense plasma core and the tenuous halo) were also present as in [24].

Let us attempt to evaluate the still photograph of the sprite shown in Fig. 6, frame #2. It was stated before that the value of the solar constant is  $1370 \text{ W/m}^2$  and that the sun emits a significant amount of the UV radiation (about 10% of its total power). Let us now assume that 1% of the solar constant is used to pump the  $\text{N}_2$  molecules to the upper excited  $\text{C}^3\Pi_u$  level.

The area of the curved surface equals to  $2\pi rh$  enables approximately the excited states in this area to participate in the creation of the sprite. Here,  $r$  is the radius of the earth ( $= 6357.72 \text{ km}$ ) and  $h$  the relative position of the sprite above the earth ( $= 70 \text{ km}$ ). As  $2\pi rh = 2.796 \cdot 10^{12} \text{ m}^2$  and with  $2\pi rh \approx \pi r_e^2$ , the corresponding equivalent radius of the circle  $r_e$  is  $943 \text{ km}$ , and the power  $P$  is

$$P = 13.7 \text{ W/m}^2 \cdot 2.796 \cdot 10^{12} \text{ m}^2 = 3.83 \cdot 10^{13} \text{ W}.$$

The wave takes  $3.14 \text{ ms}$  to travel the radial distance of  $943 \text{ km}$ . In the single pass of the wave, the energy  $E$  is

$$E = 3.14 \text{ ms} \cdot 3.83 \cdot 10^{13} \text{ W} = 1.20 \cdot 10^{11} \text{ J}. \quad (5)$$

As  $1 \text{ g}$  of TNT  $= 4 \text{ kJ}$ , the energy given in (5) is equal to  $0.030 \text{ kt}$  of TNT.

The hypersonic analogy allows us to approximate  $(R(t)/t)^2$  in (1) as the wave velocity  $v$  on power 2. Hence, for the spherical blast wave, (1) becomes

$$E = R^3 \rho_o v^2. \quad (6)$$

At the altitude of  $70 \text{ km}$ , the air density  $\rho_o$  is  $6.16 \cdot 10^{-5} \text{ kg/m}^{-3}$ . During the expansion, the spherical shock velocity  $v$  is assumed to be close to the velocity of sound in the air. At the altitude of  $70 \text{ km}$ ,  $v = 300 \text{ m/s}$ . From (5), the energy  $E = 1.20 \cdot 10^{11} \text{ J}$ . Substituting these values into (6), we get that the radius of the sprite  $R$  is  $2.787 \text{ km}$ .

In Fig. 6, frame #2, the radius of the luminous region measured as the distance from the center of the white domain at the height of  $63 \text{ km}$  to the right where we have a luminous region is circa  $3.5 \text{ km}$ . The distance of  $3.5 \text{ km}$  is of larger value than the theoretical radius of  $2.787 \text{ km}$ .

With the aid of (2), (6) can be reexamined. Inserting the volume of the sphere:  $4\pi R^3/3$  into (2), we get

$$E = k R^3 \rho_o v^2 \quad \text{where } k = 2\pi/(3(\gamma^2 - 1)). \quad (7)$$

Instead of considering the plasma to be of spherical shape, let us note the sprite shown in Fig. 9, frame #1. We see that the plasma in this picture is rather of elliptical shape. We assume that this plasma has the shape like a ‘‘bun for the burger,’’ when the bun is viewed from the side. This configuration can be presented by the oblate ellipsoid. From the center of the ellipsoid, the radius in the horizontal direction is  $R$  and the radius in the vertical direction is  $r_o$ . We take that  $R/r_o = \chi$ . For the oblate ellipsoid, (2) reads

$$E = k_1 R^3 \rho_o v^2 \quad \text{where } k_1 = k/\chi. \quad (8)$$

On the other hand, the plasma of the spherical shape can be stretched to make it longer to be like ‘‘a rugby ball.’’ In such a case, we have to consider a prolate ellipsoid. With (2), we get

$$E = k_2 R^3 \rho_o v^2 \quad \text{where } k_2 = k/\chi^2. \quad (9)$$

From Fig. 9, frame #1, we have  $\chi = R/r_o \approx 5.1$ . With this value of  $\chi$ ,  $\gamma = 1.4$  and the values of other quantities used to get  $R$  in (6), (8) gives the radius of the sprite,  $R$  to be  $3.699 \text{ km}$ , whereas (9) gives  $R$  to be  $6.367 \text{ km}$ . According to (9), the overall horizontal length of the sprite shown in Fig. 9, frame #1 could be  $12.73 \text{ km}$ .

At first glance, there are discrepancies between (6) and (7). This dilemma could be solved by noting that, in the Trinity explosion, the energy was released in about half of the sphere. This fact alters (7) so that the constant  $k$  becomes  $\pi/(3(\gamma^2 - 1))$ . For the adiabatic index in air,  $\gamma = 1.4$ , the expression:  $\pi/(3(\gamma^2 - 1)) = 1.091$ .

We understand now why G. I. Taylor had rightly stated that his constant in (1) can be approximated to be 1.

The elve shown in Fig. 6, frame #1, will be now observed. For the height of elve above the earth of  $90 \text{ km}$ , the area:  $2\pi rh = 3.5958 \cdot 10^{12} \text{ m}^2$ , and the equivalent radius of the circle  $r_e = 1069.7 \text{ km}$ , and the power  $P$  is

$$P = 13.7 \text{ W/m}^2 \cdot 3.596 \cdot 10^{12} \text{ m}^2 = 4.926 \cdot 10^{13} \text{ W}.$$

The wave takes  $3.566 \text{ ms}$  to travel the equivalent radial distance of  $1069 \text{ km}$ ; hence, the energy  $E$  is

$$E = 4.926 \cdot 10^{13} \text{ W} \cdot 3.566 \text{ ms} = 1.756 \cdot 10^{11} \text{ J}. \quad (10)$$

It could be postulated that the elve is a rapidly expanding disk of the radius  $R$  that has a constant thickness,  $h_o$  in the vertical direction. The volume of the disk is  $\pi R^2 h_o$ . With this formulation, (2) gives

$$E = k_3 R^2 h_o \rho_o v^2 \quad \text{where } k_3 = \pi/[2(\gamma^2 - 1)]. \quad (11)$$

At the altitude of  $90 \text{ km}$ , the air density  $\rho_o$  is  $2.13 \cdot 10^{-6} \text{ kg/m}^{-3}$  and the velocity of sound  $v$  is  $276 \text{ m/s}$ . From (10), the energy deposited in the elve  $E$  is  $1.756 \cdot 10^{11} \text{ J}$ . If  $h_o = 20 \text{ m}$ , (11) gives the radius of the elve,  $R$  to be  $182 \text{ km}$ .

The records show that the diameter of the expanding disk can attain the value of  $400 \text{ km}$  or even larger.

As stated before, following the detonation, the inward-going (embedded) shock is established due to the overextension of the hot gas because of the increase in the flow area and subsequent recompression near the horizontal axis. In the large body of the sprite, a number of embedded shocks can be present. For the purpose of this analysis, let us consider that a pair of imbedded shock waves is only formed at the center of the vertical axis, and not formed off the axis as indicated in Fig. 11. The imbedded shock heats the ions preferentially. Initially, if the complete equilibrium between the ions and electrons is not achieved, the embedded shock front will certainly accelerate the equilibration process.

Because of the large physical size of the sprite, the upper and lower lines of the shock waves will not be at the same potential, due to the electric field present at high altitudes. Coulomb field introduced by thundercloud charge will enhance further the difference in the potential. Since most of the electron gas is pushed toward the shock boundaries, the current path will follow the shock trajectories. The current path could be completed by the current going through the body of the

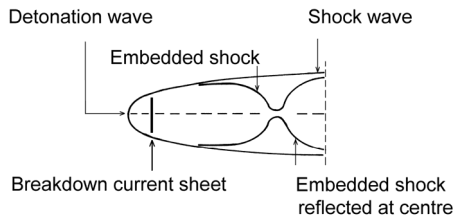


Fig. 11. Simplified shock structure of the interior of the plasma having the shape of the oblate ellipsoid. The broken lines are the axis that passes through the center of the sprite. The contact surface of the shock wave is not shown. The uniform neutral density inside the ellipsoid is assumed prior to the onset of the sprite. When the changes of the density versus the altitude are taken into account, the embedded shock center will be shifted toward the lower shock wave trajectory.

ellipsoid in the vertical direction. Instead of having uniform current flow from the shock trajectory at the top to the trajectory to the bottom, let us consider the case that the current path is completed via the narrow sheet, named “breakdown current sheet” at some distance from the detonation wavefront (Fig. 11).

At this instance, the Lorentz force is established due to the interaction between the current present at the tip of the detonation wave, and the current flowing through the “breakdown current sheet,” making the sheet to propagate toward the vertical axis. This situation corresponds to the action that is also occurring in the dense plasma focus that has Filippov type configuration. The magnetic field causes the plasma to “pinch” itself down into a filament when it reaches the center between the two imbedded shock waves.

During the propagation of the breakdown current sheet, the energy left after the laser-supported detonation is partially collected, and it is brought to the pinch where the pinch itself increases the density of the plasma rapidly, causing its temperature to increase. The total pinching time could be estimated from the snow plow model.

During the final pinch, there is a sudden decrease of the current observed commonly in all the plasma focus and/or Z-pinch experiments, as indicated well in the records of the current derivative,  $dI/dt$  vs time. The effect generates a narrow voltage spike having a negative peak. This peak creates an inductive voltage of ten or more times to appear across the pinch at the peak of the compression.

It also makes that the ionizing radiation, such as ion beams, electron beams, as well as hard and soft X-rays, will be ejected from highly compressed, high-density plasma. If the hydrogen is present in the compressed region, it is reasonable to expect that some thermonuclear reactions may take place. The theory indicates that a dense compact Z-pinch can satisfy Lawson conditions to achieve the thermonuclear fusion with a power input dependent on the enhanced stability time, or, if stable, with ohmic heating balancing vertical axial heat losses [28].

In Fig. 10, the straight 3.75-km-long filament was recorded in 2.46 ms. This filament could be interpreted as the E-beam. From the H.V. engineering point of view, this E-beam is equivalent to being the solid rod from which the classical corona discharges are initiated. If the currents during the pinch

are of smaller amplitude, the E-beam propagation path is of shorter distance, and it may not be evident in the records shown in Fig. 9, frames #2 and #3.

A large amount of energy is compressed in the small size high-density plasma during the pinch. To understand the dynamics of the plasma expansion following the pinch, the programs developed to study the effects of nuclear weapons at high altitude are needed. The following question must be answered. What is the value of the explosive charge needed to be located instead of the plasma focus to create the shock velocity of  $\sim 0.9 \cdot 10^6$  m/s in the horizontal direction from the center of the plasma focus? This velocity was determined from Fig. 10 in the time interval from 2.46 to 3.06 ms.

Furthermore, the sprite may act as the ignition point to enable the next set of the sprites to be initiated at some distance (few hundred miles) away. This implies that the TLEs events can hop from place to place as far as the distance of thousand miles away. This process will occur under the condition that the number density of the excited nitrogen states has reached sufficiently large value to facilitate the  $N_2$  laser beam generation in the mesosphere. In addition, the contribution by the energy departed to the  $N_2$  molecules by the solar wind needs to be considered in the evolution of the energy departed to the development of the sprite.

## VIII. CONCLUSION

In this paper, an attempt is made to present the unified photograph of some aspects of the electrical discharges taking place in the laboratory, and the discharges occurring at high altitude. The emphasis is made to the creation of the laser emission, to the dynamics of the laser-supported detonation as well as to the processes leading to the formation of the dense plasma focus, and to the processes occurring consequently thereafter.

Fig. 4 shows that the pulses of long ( $< 3 \mu\text{s}$ ) duration and of short ( $\approx 10$  ns) duration have been generated in the laboratory. The photodiode registered both the spontaneous and the stimulated (laser) emission in the  $337 \pm 5$  nm spectral range. Fig. 5 depicts that the  $N_2$  laser emission predominates in the experimental setup used.

Using the gas dynamics consideration, an attempt was made to account for the energy balance of the discharges at high altitude. For the elve shown in Fig. 6, frame #1 and the sprites shown in Fig. 6, frames #2 and Fig. 9, the evaluation was attempted.

Fig. 7 indicates that, because of the beams emerging apparently from the explosion of the transformer, the discharge processes have been initiated in the sky. This discharge was named the “Crepuscular Twilight in the Sky of New York.” Without the beams, most probably the sky over New York would have been uneventful that day.

The concept herewith proposed should hold for the “mysterious bright flash” as shown in Fig. 8.

The Tunguska event still remains an enigma. Whether or not Nikola Tesla did trigger the Tunguska event remains still an open question. Because of his upbringing/beliefs, Tesla could not make such a claim. He argued for a long time that he

was mainly interested to harness Sun's energy stored in the mesosphere/ionosphere for the benefit of mankind, an idea that would come to obsess him in the later years of his life.

The claims that Nikola Tesla have obtained the first successful laser-supported thermonuclear experiment by triggering the fusion process with his generator located at Wardenclyffe Tower, on Long Island, New York and, creating the super-weapon, are still an exaggeration. We do not have proof. Fig. 8 shows the sign of encouragement to continue with the research. After all, the most puzzling aspect is Tesla's own belief that he could generate the Tunguska-like event at the location of his choice.

Nikola Tesla was the key founder of alternating current, the electrical distribution system throughout the world and the motors it powered. We have to honor Nikola Tesla for being one of the few individuals whose vision profoundly changed the world for the better with his research efforts.

#### REFERENCES

- [1] A. V. Martinez and V. Aboites, "High-efficiency low-pressure Blumlein nitrogen laser," *IEEE J. Quantum Electron.*, vol. 29, no. 8, pp. 2364–2370, Aug. 1993.
- [2] D. Basting, F. P. Schäfer, and B. Steyer, "A simple, high power nitrogen laser," *Opt.-Electron.*, vol. 4, no. 1, pp. 43–49, Jan. 1972.
- [3] V. F. Tarasenko, "Efficiency of a nitrogen UV laser pumped by a self-sustained discharge," *Quantum Electron.*, vol. 31, no. 6, pp. 489–494, Jun. 1991.
- [4] M. Richardson, A. Alcock, K. Leopold, and P. Burtyn, "A 300-J multigigawatt CO<sub>2</sub> laser," *IEEE J. Quantum Electron.*, vol. QE-9, no. 2, pp. 236–242, Feb. 1973.
- [5] A. J. Beaulieu, "Transversely excited atmospheric pressure CO<sub>2</sub> lasers," *Appl. Phys. Lett.*, vol. 16, pp. 504–505, Jun. 1970.
- [6] M. M. Kekez, "Laser and microwave generations in nitrogen," *IEEE Trans. Plasma Sci.*, vol. 46, no. 3, pp. 545–555, Mar. 2018.
- [7] M. Füllekrug, E. A. Mareev, and M. J. Rycroft, *Sprites, Elves and Intense Lightning Discharges*. Corsica, France: Springer, 2004.
- [8] (Jan. 24, 2018) *Tunguska Effect*. [Online]. Available: [https://en.wikipedia.org/wiki/Tunguska\\_event](https://en.wikipedia.org/wiki/Tunguska_event)
- [9] Y. P. Raizer, G. M. Milikh, and M. N. Shneider, "Streamer-and leader-like processes in the upper atmosphere: Models of red sprites and blue jets," *J. Geophys. Res. Space Phys.*, vol. 115, no. A7, 2010. Art. no. A00E42. doi: [10.1029/2009JA014645](https://doi.org/10.1029/2009JA014645).2010.
- [10] U. S. Inan, "Lightning effects at high altitudes: Sprites, elves, and terrestrial gamma ray flashes," *Comp. Rendus Physique*, vol. 3, pp. 1411–1421, Dec. 2002.
- [11] J. M. Meek and J. D. Craggs, *Electrical Breakdown of Gases*. Hoboken, NJ, USA: Wiley, 1978.
- [12] L. P. Babich, T. V. Loiko, and V. A. Tsukerman, "High-voltage nanosecond discharge in a dense gas at a high overvoltage with runaway electrons," *Sov. Phys. Uspekhi*, vol. 33, no. 7, pp. 521–540, Jul. 1990.
- [13] G. M. Milikh, K. Papadopoulos, and C. L. Chang, "On the physics of high altitude lightning," *Geophys. Res. Lett.*, vol. 22, no. 2, pp. 85–88, Jan. 1995.
- [14] D. D. Sentman and E. M. Westort, "Observations of upper atmospheric optical flashes recorded from an aircraft," *Geophys. Res. Lett.*, vol. 20, no. 24, pp. 2857–2860, Dec. 1993.
- [15] A. Einstein, "Zur Quantentheorie der Strahlung," *Phys. Zeitschrift*, vol. 18, pp. 121–128, 1917. [Online]. Available: <http://adsabs.harvard.edu/abs/1917PhyZ..18.121E>
- [16] M. M. Kekez, "Simulation of nikola tesla atmospheric (maser) discharges," *IEEE Trans. Plasma Sci.*, vol. 43, no. 10, pp. 3608–3614, Oct. 2015.
- [17] M. Cheney and R. Uth, *Tesla, Master of Lightning*. New York, NY, USA: Barnes & Noble, 1999.
- [18] (Jan. 24, 2019). *Blast Wave, Derivation of G. I. Taylor's Similarity Solution*. [Online]. Available: <http://www.atmos.physics.utoronto.ca/people/codoban/PHY138/Mechanics/dimensional.pdf>
- [19] G. I. Taylor, "The formation of a blast wave by a very intense explosion I. Theoretical discussion," *Proc. Roy. Soc. London, Ser. A*, vol. 201, no. 1065, pp. 159–186, Mar. 1950.
- [20] P. Yu Raizer, "Heating of a gas by a powerful light pulse," *Sov. Phys. JETP*, vol. 21, no. 5, pp. 1009–1017, Nov. 1965.
- [21] M. M. Kekez and P. Savic, "A hypersonic interpretation of the development of the spark channel in gases," *J. Phys. D, Appl. Phys.*, vol. 7, no. 4, pp. 620–628, Mar. 1974.
- [22] M. M. Kekez and P. Savic, "Contribution to continuous leader channel development," in *Proc. NATO Adv. Study Inst. Elect. Breakdown Discharges Gases*, Les Arcs, France, Jun./Jul. 1981, pp. 419–454.
- [23] A. Alcock, C. Demichelis, K. Hamal, and B. Tozer, "A mode-locked laser as a light source for Schlieren photography," *IEEE J. Quantum Electron.*, vol. QE-4, no. 10, pp. 593–597, Oct. 1968.
- [24] E. V. George, G. Bekefi, and B. Ya'akobi, "Structure of the plasma fireball produced by a CO<sub>2</sub> laser," *Phys. Fluids*, vol. 14, no. 12, pp. 2708–2713, Dec. 1971.
- [25] M. Richardson and A. Alcock, "An interferometric study of CO<sub>2</sub>-laser-produced sparks," *IEEE J. Quantum Electron.*, vol. QE-9, no. 12, pp. 593–597, Dec. 1973.
- [26] S. A. Ramsden and P. Savic, "A radiative detonation model for the development of a laser-induced spark in air," *Nature*, vol. 203, no. 4941, pp. 1217–1219, Sep. 1964.
- [27] S. A. Cummer, N. Jaugey, J. Li, W. A. Lyons, T. E. Nelson, and E. A. Gerken, "Submillisecond imaging of sprite development and structure," *Geophys. Res. Lett.*, vol. 33, Feb. 2006, Art. no. L04104. doi: [10.1029/2005GL024969](https://doi.org/10.1029/2005GL024969), 2006.
- [28] M. G. Haines, "Dense plasma in Z-pinch and the plasma focus," *Philosophic Trans. Roy. Soc. A*, vol. 300, no. 1456, pp. 649–663, Apr. 1981. doi: [10.1098/rsta.1981.0093](https://doi.org/10.1098/rsta.1981.0093)



**Mladen M. Kekez** was born in 1941. He received the Dipl.-Ing. degree from the University of Belgrade, Belgrade, Serbia, in 1965, and the Ph.D. degree from the University of Liverpool, Liverpool, U.K. in 1968.

From 1971 to 1972 and 1974 to 2002, he was with the National Research Council of Canada, Ottawa, ON, Canada, where he was involved in research and development on gas discharges, pulsed power technology, plasma fusion related experiments, biophysics, and fluid dynamics. From 1972 to 1974,

he was at the University of Alberta, Edmonton, AB, Canada, where he was involved in CO<sub>2</sub> lasers. In 2002, he formed the company High-Energy Frequency Tesla Inc., Ottawa, ON, Canada, where he was involved in research and development. One of his current research and development is in the high-power microwave (HPM)/laser radiation in the air, other gases, and gas mixture.